IEEE Access
Multidisciplinary | Rapid Review | Open Access Journal

Received September 8, 2021, accepted September 29, 2021, date of publication October 4, 2021, date of current version October 12, 2021.

Digital Object Identifier 10.1109/ACCESS.2021.3117446

An Exact Error Analysis of Multi-User RC/MRC Based MIMO-NOMA-VLC System With Imperfect SIC

VIPUL DIXIT, (Student Member, IEEE), AND ATUL KUMAR, (Member, IEEE)
Department of Electronics and Communication, PDPM-Indian Institute of Information Technology, Design and Manufacturing, Jabalpur, Jabalpur 482005, India
Corresponding author: Atul Kumar (atul.kumar@iiitdmj.ac.in)

ABSTRACT Visible Light Communication (VLC) has appeared as a breakthrough technology for beyond 5G networks by delivering a broad license free spectrum. In this paper, multiple input multiple output (MIMO) technique is implemented with non-orthogonal multiple access (NOMA-VLC) system in order to develop a robust error-free high rate network for a multi-user scenario. In particular, a generalized multi-user MIMO-NOMA-VLC system with $M \times N$ line-of-sight (LOS) links per user is proposed which adopts on-off keying (OOK) modulation for data transmission. A novel closed form expression of probability of error for the proposed system is derived considering a practical scenario of imperfect successive interference cancellation (SIC). This paper also presents the detailed analysis of a three user 2×2 MIMO-NOMA-VLC system and an exact closed form expression of probability of error of this system is derived. The three user 2×2 MIMO-NOMA-VLC system completely outperforms the single input single output (SISO) NOMA-VLC system with same set of parameters. The error performance of the proposed system enhances as the number of photo detectors (PDs) at each user increases. A three user 2×2 MIMO-NOMA-VLC system ensures the best performance at the power allocation co-efficient of 0.3. The error performance of the proposed system is investigated for the parameters of interest, i.e., distance between the transmitting LEDs and distance between the receiving PDs at each user terminal. The derived probability of error expressions are verified with the simulation results.

INDEX TERMS Visible light communication (VLC), non-orthogonal multiple access (NOMA), multiple input multiple output (MIMO), bit-error-rate (BER).

I. INTRODUCTION

It is expected that there will be 13.1 billion wireless connected devices by the year 2023 due to increase in global connectivity over 70 percent of population [1]. Thus accommodation of such a huge traffic is almost impossible for the radio frequency spectrum. Visible light communication (VLC) offers a license-free wide spectrum of 430 THz to 790 THz and thus emerges as a breakthrough technology for beyond 5G networks [2]. VLC offers a military grade security as being an optical wireless technique. Besides, VLC offers several merits such as straightforwardness in implementation, prolonged life, no eye hazard, low power operation and no electromagnetic interference and hence, finds various popular applications in the areas such as Li-Fi, radiation sensitive areas, optical-camera communication, indoor positioning system, and vehicular communication, etc. [3]–[5].

In recent times, many multiple access techniques, i.e., code division multiple access (CDMA), orthogonal frequency division multiple access (OFDMA) and interleave division multiple access (IDMA), have been applied with VLC systems to attain high rate and low error performance [5]–[7]. Recently, a new multiple access technique, i.e., non-orthogonal multiple access (NOMA), attracted the researchers by offering high spectral and energy efficiency, enhanced capacity and superior outage probability [8]. In NOMA, the users are multiplexed in power domain using multiuser superposition transmit (MUST) technique [9]. For decoding propose, a multi-user detection technique, i.e., successive interference cancellation (SIC), is used at the receiver. The performance of multi user downlink NOMA is investigated in [10], however, it is suggested in [11]

The associate editor coordinating the review of this manuscript and approving it for publication was Bong Jun David Choi.

that for better practical suitability, NOMA should be implemented with two users. In [12], it is shown that for large user count, NOMA attains higher system capacity than that of time division multiple access (TDMA) over VLC channel. An experimental demonstration of single carrier (SC) based NOMA-VLC system is presented in [13] which offers an enhanced error performance compared to OFDM-VLC system. The symbol error rate (SER) performance of NOMA-VLC system with square M-QAM modulation is studied in [14]. The error performance of NOMA-VLC system with different modulation techniques, i.e., M-PSK, M-QAM and M-PAM, is analyzed and compared in [15]. In [16], the BER performance of NOMA-VLC system with on-off keying (OOK) modulation is studied using maximum likelihood (ML) detection. The BER Analysis of NOMA-VLC System with Imperfect SIC and CSI is presented in [17]. In [18], it is shown that constellations partitioning coding (CPC) technique can mitigate the effect of imperfect SIC in QAM modulated NOMA-VLC system.

Multiple input multiple output (MIMO) technique is widely used in VLC systems in order to improve the system capacity and coverage [19]–[21]. In [19], performance of both non-imaging and imaging MIMO-VLC system is analyzed and compared. The error performance of angular diversity receiver based MIMO-VLC system is analyzed in [20]. In [21], various MIMO techniques are applied to VLC systems and their performance are compared. However, a very limited research work investigates the performance of MIMO based NOMA-VLC system [22], [23]. In [22], a new power allocation strategy for MIMO-NOMA-VLC system is presented which improves the sum-rate to a large extent. A novel precoder design for non-linear VLC channel is proposed in [23] to improve the performance of MIMO-NOMA-VLC system.

Most of the research works reported in literature focus on the outage and sum rate analysis of MIMO-NOMA-VLC system [22], [23]. However, to the best of our knowledge, no research work which investigates the error performance of MIMO-NOMA-VLC system is reported in the literature.

In this paper, the error performance of multi-user downlink MIMO-NOMA-VLC system is analyzed over line-of-sight (LOS) channel. Specifically, OOK modulation is used for signal transmission and a fixed power allocation strategy is considered for NOMA implementation. The main contributions of the paper are enlisted below

- In particular, a generalized MIMO-NOMA-VLC system with K users is considered and without loss of generality, the performance analysis of k^{th} user, $1 \leq k \leq K$, is presented. Thereafter, a three user MIMO-NOMA-VLC system is adopted to investigate the error performance of the users in detail.
- In order to improve the error performance, MIMO technique is implemented with the NOMA-VLC system. Specifically, repetition coding (RC) is employed at the transmitter and maximum ratio combining (MRC) is adopted at the receiver to get the benefit of diversity combining.
- The exact closed form expressions of the probability of error of the generalized multi-user MIMO-NOMA-VLC system are derived in the presence of perfect and imperfect SIC. Further, this analysis is extended for a three user MIMO-NOMA-VLC system.
- The error performance of the proposed multi user MIMO-NOMA-VLC system is compared with that of single input single output (SISO) NOMA-VLC system of [16].
- The performance of the proposed system is investigated for the various parameters of interest. The derived closed form expressions are verified with the simulation results.

The remaining paper is organized as follows: Section II describes the system model. Section III and Section IV present the performance analysis of generalized MU-MIMO-NOMA-VLC system and three user MIMO-NOMA-VLC system, respectively. The results are discussed in Section V and Section VI concludes the paper.

II. SYSTEM MODEL

An intensity modulation and direct detection (IM/DD) based indoor multi-user downlink MIMO-NOMA-VLC system with N LED's as transmitter and M photo detector's (PD's) at each user as receiver is under consideration. The block diagram of the considered system is shown in Fig. 1. A room with typical dimension of (d, d, h) m is considered. The transmitter is located at the center of the roof wherein, the n^{th} LED, i.e., $1 \leq n \leq N$, is located with the co-ordinates of (x_n, y_n, h) m, and the receivers are located on the floor with the co-ordinates $\left(x_m^k, y_m^k, h_1\right)$ m, $1 \leq k \leq K, 1 \leq m \leq M$, where h_1 is the height of receivers above the ground. In this analysis only LOS path is considered, as the power received through Non-LOS path is much lower than that of LOS path [19], [24], [25]. The direct current (DC) channel gain of LOS path between n^{th} LED, $1 \leq n \leq N$, and m^{th} PD, $1 \leq m \leq M$, of the k^{th} user, $1 \leq k \leq K$, is given by [2], [26]

$$h_{mn}^k = \frac{A_m}{d_{mn}^2} R\left(\phi_{mn}\right) T\left(\psi_{mn}\right) g\left(\psi_{mn}\right) \cos\left(\psi_{mn}\right), \qquad (1)$$

where A_m is the active area of m^{th} PD, d_{mn} is the distance between n^{th} LED and m^{th} PD, ϕ_{mn} is the angle of emission from n^{th} LED to m^{th} PD, ψ_{mn} is angle of incidence at m^{th} PD from n^{th} LED, $T\left(\psi_{mn}\right)$ is the optical filter gain of the m^{th} PD from n^{th} LED, $g\left(\psi_{mn}\right) = n^2/\sin^2 \psi_c, 0 \leq \psi_{mn} \leq \psi_c$, is the gain of optical concentrator with refractive index n and ψ_c is the field of view (FOV) of the PD and $R\left(\phi_{mn}\right)$ is the radiation intensity of the LED with Lambertian pattern and can be given as [26]

$$R\left(\phi_{mn}\right) = \begin{cases} \dfrac{(\ell+1)}{2\pi} \cos^{\ell} \phi_{mn}, & for\ \phi_{mn} \in [-\pi/2, \pi/2] \\ 0, & otherwise, \end{cases} \qquad (2)$$

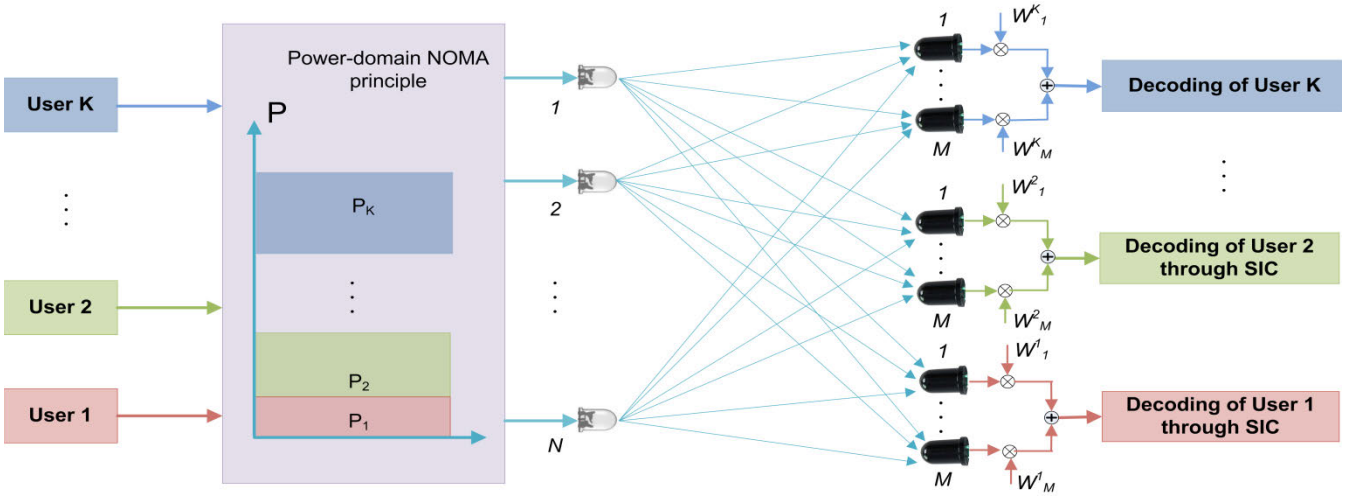

FIGURE 1. System model of MU-MIMO-NOMA-VLC system over LOS channel.

where $\ell = -\ln 2/\ln\left(\cos\phi_{1/2}\right)$ is the Lambertian order related to the semi-angle at half power of LED, $\phi_{1/2}$.

The $M \times N$ channel matrix for MIMO-NOMA-VLC system at the k^{th} user is given by

$$H^k = \begin{bmatrix} h^k_{11} & h^k_{21} & \vdots & h^k_{M1} \\ h^k_{12} & h^k_{22} & \vdots & h^k_{M2} \\ \dots & \dots & \ddots & \dots \\ h^k_{1N} & h^k_{2N} & \vdots & h^k_{MN} \end{bmatrix}, \tag{3}$$

where h^k_{mn}, $1 \le m \le M$, $1 \le n \le N$, is defined in (1).

A. REPETITION CODING (RC)

At the transmitter, RC is used to gain the benefit of transmit diversity. In RC, the signal is transmitted from all the LEDs simultaneously [27]. Thus, in RC, $x_1 = x_2 = \ldots = x_N$ holds, where x_n, $1 \le n \le N$, is the transmitted signal from n^{th} LED. At the receiver, the optical power emitted from multiple LEDs is combined constructively. Thus, the equivalent received optical power at m^{th} PD is given as $P_m = \sum_{n=1}^{N} \frac{P_t}{N} h^k_{mn} = P_{avg} h^k_m$, where P_t is the total transmit power, $P_{avg} = P_t/N$ is the average transmit power per LED and $h^k_m = \sum_{n=1}^{N} h^k_{mn}$ is the equivalent channel gain at the m^{th} PD.

Thus, the received signal at m^{th} PD of the k^{th} user is given by

$$r^k_m = h^k_m R_p x + n^k_m, \tag{4}$$

where R_p is the responsivity of PD, x is the transmitted signal from LED, n^k_m is the additive white Gaussian noise (AWGN) at m^{th} PD of the k^{th} user with zero mean and σ^2_n variance.

As n^k_m consists of shot and thermal noise, σ^2_n can be written as $\sigma^2_n = \sigma^2_{shot} + \sigma^2_{thermal}$, where $\sigma^2_{shot} = \left[2qI_bI_2W + 2qR_rP_jW\right]$ and $\sigma^2_{thermal} = 8\pi kT_aAI_2W^2\eta/G + 16\pi^2kT_aA^2I_3W^3\eta^2\Gamma/g_m$ are the variance of shot and thermal noise, respectively, q is charge of electron, W is bandwidth of noise which is equal to bandwidth of modulation, $I_b = 5100\mu A$ is background current under direct exposure to sunlight, P_m is equivalent received optical power at the m^{th} PD and $I_2 = 0.562$ is noise bandwidth factor, k is Boltzmann's constant, $T_a = 295K$ is absolute temperature, $G = 10$ is open loop voltage gain, $\eta = 112pF/cm^2$ is fixed capacitance of PD per unit area, A is PD's active area, $\Gamma = 1.5$ is channel noise factor of FET, $g_m = 30mS$ is transconductance of FET, and $I_3 = 0.0868$ [1], [28].

B. MAXIMUM RATIO COMBINING (MRC)

At the receiver, MRC is used to gain the benefit of receiver diversity. In MRC, the received signals are co-phased followed by weight assignment and addition.

The weights are assigned according to the knowledge of channel gain of the respective PD's at k^{th} user so that the output SNR can be maximized. Thus, the output of MRC combiner at k^{th} user is given by

$$\begin{aligned} y_k &= \sum_{m=1}^{M} w^k_m r^k_m \\ &= \sum_{m=1}^{M} \left(h^k_m\right)^2 R_p x + n^k, \end{aligned} \tag{5}$$

where $w^k_m = h^k_m$ is the assigned weight at m^{th} PD of k^{th} user and n^k is weighted noise at k^{th} user.

C. NOMA-VLC SIGNALING SCHEME

Without loss of generality, the ordering of the users is performed according to the sum of M optical channel gains received by different PD's at a particular user as $\sum_{m=1}^{M} \left|h^1_m\right| \ge \sum_{m=1}^{M} \left|h^2_m\right| \ge \cdots \ge \sum_{m=1}^{M} \left|h^K_m\right|$. According to the NOMA

principle, for successful implementation of SIC, the user with the lower channel gain is assigned with a higher optical transmission power. In this paper, fixed power strategy is considered in which the power assigned to k^{th} user is $P_k = \alpha P_{k+1}$, where α is the power allocation co-efficient with $0 < \alpha < 1$ and $\sum_{k=1}^{K} P_k = P_{avg}$.

Using NOMA principle, the LED transmits the OOK modulated symbols, s_l, $l \in \{1, \ldots, K\}$, intended for K users after superimposing them in power domain as $x = \sum_{l=1}^{K} 2P_l s_l$, where factor 2 is used to keep the average transmit power as P_{avg} because there is no signal transmission for bit '0'.

III. PERFORMANCE ANALYSIS

The received signal at k^{th} user after the MRC combining is given by

$$y_k = R_p \left(\sum_{l=1}^{K} 2P_l s_l \right) \left(\sum_{m=1}^{M} \left(h_m^k \right)^2 \right) + n^k. \tag{6}$$

For the simplicity of representation, equivalent channel gain at the k^{th} user terminal is considered as $h_k = \sum_{m=1}^{M} \left(h_m^k \right)^2$. The probability of error for the direct detection of the j^{th}, $k \leq j \leq K$, user at k^{th} user terminal can be written as

$$P_e^{kj} = \sum_{i=0}^{2^j-1} P\left(y_k \neq s_j \left| s_1^i, s_2^i, \ldots, s_j^i \right. \right) P\left(s_1^i, s_2^i, \ldots, s_j^i \right), \tag{7}$$

where $\left(s_1^i, s_2^i, \ldots, s_j^i \right)$ is the i^{th} combination of the symbols of users and i ranges from 0 to $2^j - 1$.

For equi-probable occurrence of symbols, the probability of error is given by

$$P_e^{kj} = \frac{1}{2^j} \sum_{i=0}^{2^j-1} P\left(y_k \neq s_j \left| s_1^i, s_2^i, \ldots, s_j^i \right. \right), \tag{8}$$

where y_k is defined in (6) and is a Gaussian distributed random variable with the probability density function (PDF) $f_{y_k}(z) = \frac{1}{\sqrt{2\pi\sigma_k^2}} e^{-(z-m_k)^2/2\sigma_k^2}$, with $m_k = 2R_p h_k \sum_{l=1}^{K} P_l s_l$ and $\sigma_k^2 = h_k \sigma_n^2$.

It is to be noted that the threshold for symbol detection of j^{th} user at k^{th} user terminal is $i_{th_{k_j}} = 2R_p P_j h_k / 2$, and thus, the expression for the probability of error using (8) can be given as

$$P_e^{kj} = \frac{1}{2^j} \left[\sum_{i=0}^{2^{j-1}-1} Q\left(\frac{R_p \sqrt{h_k}}{\sigma_n} \left(P_j - \sum_{l=1}^{j-1} 2P_l s_l^i \right) \right) + \sum_{i=0}^{2^{j-1}-1} Q\left(\frac{R_p \sqrt{h_k}}{\sigma_n} \left(P_j + \sum_{l=1}^{j-1} 2P_l s_l^i \right) \right) \right]. \tag{9}$$

The decoding of extreme far user does not require the involvement of SIC and hence, the probability of error for the extreme far user can be obtained by substituting, $k = j = K$ in (9).

The decoding of all users except the extreme far user can be performed with the implementation of SIC. Thus, the output signal at the k^{th} user, $k \neq K$, is given by

$$\widehat{y_k} = y_k - \sum_{l=k+1}^{K} 2R_p h_k P_l \widehat{s_l}, \tag{10}$$

where $\widehat{y_k}$ is Gaussian distributed with mean $\widehat{m_k} = 2R_p h_k \left(\sum_{l=1}^{K} P_l s_l - \sum_{l=k+1}^{K} P_l \widehat{s_l} \right)$ and variance $\widehat{\sigma}_k^2 = h_k \sigma_n^2$, and $\widehat{s_l}$ is the decoded symbol of the l^{th} user, $(k+1) \leq l \leq K$.

The probability of error of the k^{th} user is given by

$$P_e^k = \sum_{v=1}^{2^{K-k}} P\left(e_k^{(v)} \left| e_{k+1}^{(v)}, e_{k+2}^{(v)}, \ldots, e_K^{(v)} \right. \right), \tag{11}$$

where v denotes all the possible error combinations at the k^{th} user which includes error in self-decoding and the errors generated during the SIC implementation for $(k+1)$ to K^{th} user. The self-decoding error at k^{th} user is arised, when $\widehat{s_k} \neq s_k$ and is denoted as $e_k^{(v)} = 1$. Similarly, the correct self-decoding at k^{th} user is denotes as $e_k^{(v)} = 0$, when $\widehat{s_k} = s_k$.

For further solution of (11), two cases may be possible; perfect SIC decoding and imperfect SIC decoding.

A. PERFECT SIC DECODING

For perfect SIC decoding, $\widehat{s_l} = s_l$, where $(k+1) \leq l \leq K$. Thus the probability of error at the k^{th} user for this case is given by substituting $v = 1$ in (11) as

$$\begin{aligned} P_{e,1}^k &= P\left(e_k^1 = 1 \right) \prod_{l=k+1}^{K} P\left(e_l^1 = 0 \right) \\ &= P_e^{kj} \big|_{k=j} \prod_{l=k+1}^{K} \left(1 - P_e^{kl} \right), \end{aligned} \tag{12}$$

where P_e^{kl} is the probability of error of the l^{th} user, $(k+1) \leq l \leq K$, decoded at the k^{th} user terminal and $P_e^{kj} \big|_{k=j}$ is the probability of error of the self-decoding at the k^{th} user terminal.

Eq. (12) can be further solved by substituting the appropriate values in (9).

B. IMPERFECT SIC DECODING

For imperfect SIC decoding, $\widehat{s_l} \neq s_l$, where $(k+1) \leq l \leq K$. Thus, the probability of error at the k^{th} user for this case is given by substituting $2 \leq v \leq 2^{K-k}$ in (11) as

$$P_{e,2}^k = \sum_{v=2}^{2^{K-k}} P\left(e_k^{(v)} \left| e_{k+1}^{(v)}, e_{k+2}^{(v)}, \ldots, e_K^{(v)} \right. \right), \tag{13}$$

where $P\left(e_k^{(v)} \left| e_{k+1}^{(v)}, e_{k+2}^{(v)}, \ldots e_K^{(v)}\right.\right)$ is the probability of error of the v^{th} error combination at the k^{th} user, and can be given as

$$\begin{aligned} &P\left(e_k^{(v)} \left| e_{k+1}^{(v)}, e_{k+2}^{(v)}, \ldots, e_K^{(v)}\right.\right) \\ &\quad = \sum_i P\left(\widehat{y_k} \neq s_k \left| s_1^i, s_2^i, \ldots, s_k^i, \widehat{s_{k+1}^i}, \ldots, \widehat{s_K^i}\right.\right) \\ &\qquad \times P\left(\widehat{s_{k+1}^i} \neq s_{k+1} \left| s_1^i, s_2^i, \ldots, s_k^i, s_{k+1}^i, \ldots, \widehat{s_K^i}\right.\right) \\ &\qquad \times P\left(\widehat{s_K^i} \neq s_K \left| s_1^i, s_2^i, \ldots, s_k^i, s_{k+1}^i, \ldots, s_K^i\right.\right) \\ &\qquad \times P\left(s_1^i\right) P\left(s_2^i\right) \ldots P\left(s_k^i\right) \ldots P\left(s_K^i\right), \end{aligned} \tag{14}$$

where i denotes the number of possible symbol combinations. The error probability of the k^{th} user can be obtained using (11), (12) and (14) as

$$P_e^k = P_{e,1}^k + P_{e,2}^k. \tag{15}$$

IV. ANALYSIS OF THREE USER SCENARIO

This section presents the detailed probability of error analysis for a three user MIMO-NOMA-VLC system. In particular, three users, i.e., U_1, U_2 and U_3, are considered as shown in Fig. 2. The users are ordered according to their equivalent channel gains as $U_1 > U_2 > U_3$. The fixed power allocation is adopted for NOMA implementation as discussed in Section II (C).

A. PERFORMANCE OF EXTREME FAR USER (U_3)

The probability of error for U_3 can be calculated directly by substituting $k = j = 3$ in (9) as

$$\begin{aligned} P_e^3 = P_e^{3_3} = \frac{1}{2^3}\Bigg[&\sum_{i=0}^{3} Q\left(\frac{R_p\sqrt{h_3}}{\sigma_n}\left(P_3 - \sum_{l=1}^{2} 2P_l s_l^i\right)\right) \\ &+ \sum_{i=0}^{3} Q\left(\frac{R_p\sqrt{h_3}}{\sigma_n}\left(P_3 + \sum_{l=1}^{2} 2P_l s_l^i\right)\right)\Bigg]. \end{aligned} \tag{16}$$

It is to be noted that there will be eight possible combinations of symbols at U_3. Thus, an exact probability of error expression for U_3 can be obtained using (16) as

$$\begin{aligned} P_e^3 = P_e^{3_3} = \frac{1}{8}\big[&2Q\left(\Upsilon_3 P_3\right) + Q\left(\Upsilon_3\left(P_3 - 2P_1\right)\right) \\ &+ Q\left(\Upsilon_3\left(P_3 + 2P_1\right)\right) + Q\left(\Upsilon_3\left(P_3 - 2P_2\right)\right) \\ &+ Q\left(\Upsilon_3\left(P_3 + 2P_2\right)\right) + Q\left(\Upsilon_3\left(P_3 - 2P_1 - 2P_2\right)\right) \\ &+ Q\left(\Upsilon_3\left(P_3 + 2P_1 + 2P_2\right)\right)\big], \end{aligned} \tag{17}$$

where $\Upsilon_3 = R_p\sqrt{h_3}/\sigma_n$.

B. PERFORMANCE OF MIDDLE USER (U_2)

The probability of error for the middle user, i.e., $k = 2$, can be obtained using (15) as

$$P_e^2 = P\left(e_2^{(1)} = 1 \left| e_3^{(1)} = 0\right.\right) + P\left(e_2^{(2)} = 1 \left| e_3^{(2)} = 1\right.\right), \tag{18}$$

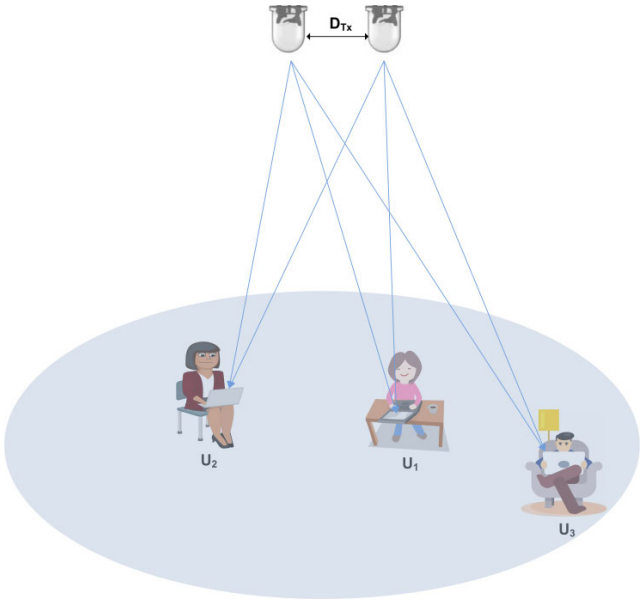

FIGURE 2. Three user based MIMO-NOMA-VLC system.

where $P\left(e_2^{(1)} = 1 \left| e_3^{(1)} = 0\right.\right)$ denotes the probability of error for perfect SIC case and $P\left(e_2^{(2)} = 1 \left| e_3^{(2)} = 1\right.\right)$ denotes the probability of error for imperfect SIC case. The derivations of $P\left(e_2^{(1)} = 1 \left| e_3^{(1)} = 0\right.\right)$ and $P\left(e_2^{(2)} = 1 \left| e_3^{(2)} = 1\right.\right)$ are given below.

In perfect SIC case, U_3 is decoded without an error at U_2 and hence, the interference related to U_3 will be cancelled out perfectly. Thus, the probability of error in this case can be given using (12) as

$$\begin{aligned} P\left(e_2^{(1)} = 1 \left| e_3^{(1)} = 0\right.\right) &= P\left(e_2^{(1)} = 1\right) P\left(e_3^{(1)} = 0\right) \\ &= P_e^{2_2}\left(1 - P_e^{2_3}\right), \end{aligned} \tag{19}$$

where $P_e^{2_2}$ is the probability of error of self-decoding at U_2 and $P_e^{2_3}$ is the probability of error of U_3 decoded at U_2. The probabilities $P_e^{2_2}$ and $P_e^{2_3}$ can be obtained directly by substituting the appropriate value of k and j in (9), and are given in (20) and (21), respectively, where $\Upsilon_2 = R_p\sqrt{h_2}/\sigma_n$.

$$\begin{aligned} P_e^{2_2} = \frac{1}{4}\big[&2Q\left(\Upsilon_2 P_2\right) + Q\left(\Upsilon_2\left(P_2 - 2P_1\right)\right) \\ &+ Q\left(\Upsilon_2\left(P_2 + 2P_1\right)\right)\big]. \end{aligned} \tag{20}$$

$$\begin{aligned} P_e^{2_3} = \frac{1}{8}\big[&2Q\left(\Upsilon_2 P_3\right) + Q\left(\Upsilon_2\left(P_3 - 2P_1\right)\right) \\ &+ Q\left(\Upsilon_2\left(P_3 + 2P_1\right)\right) + Q\left(\Upsilon_2\left(P_3 - 2P_2\right)\right) \\ &+ Q\left(\Upsilon_2\left(P_3 + 2P_2\right)\right) + Q\left(\Upsilon_2\left(P_3 - 2P_1 - 2P_2\right)\right) \\ &+ Q\left(\Upsilon_2\left(P_3 + 2P_1 + 2P_2\right)\right)\big]. \end{aligned} \tag{21}$$

In imperfect SIC case, U_3 is decoded with an error and accordingly, an additional interference related to incorrect decoding of U_3, i.e., $\widehat{s_3} \neq s_3$, is added to the received signal as in (10). Thus, the probability of error in this case can be

calculated using (14) as

$$P\left(e_2^{(2)}=1\left|e_3^{(2)}=1\right.\right)=\sum_{i=0}^{7}\Big[P\left(\widehat{y_2}\neq s_2\left|s_1^i\,,s_2^i,\widehat{s_3^i}\right.\right)P\left(\widehat{s_3^i}\neq s_3\left|s_1^i\,,s_2^i,s_3^i\right.\right)P\left(s_1^i\right)P\left(s_2^i\right)P\left(s_3^i\right)\Big]. \quad (22)$$

By substituting the symbol values in different symbol combinations, and using direct detection method, Eq. (22) can be further solved as in (23), as shown at the bottom of the page.

C. PERFORMANCE OF NEAREST USER (U_1)

The probability of error for the nearest user, i.e., $k=1$, can be obtained using (15) as

$$P_e^1=P\left(e_1^{(1)}=1\left|e_2^{(1)}=0,e_3^{(1)}=0\right.\right)+\sum_{v=2}^{4}P\left(e_1^{(v)}\left|e_2^{(v)},e_3^{(v)}\right.\right), \quad (24)$$

where $P\left(e_1^{(1)}=1\left|e_2^{(1)}=0,e_3^{(1)}=0\right.\right)$ denotes the probability of error for perfect SIC case and $\sum_{v=2}^{4}P\left(e_1^{(v)}\left|e_2^{(v)},e_3^{(v)}\right.\right)$ denotes the probability of error for imperfect SIC cases.

For perfect SIC case, the probability of error expression can be obtained using (12) as

$$\begin{aligned}P\left(e_1^{(1)}=1\left|e_2^{(1)}=0,e_3^{(1)}=0\right.\right)&=P\left(e_1^{(1)}=1\right)P\left(e_2^{(1)}=0\right)P\left(e_3^{(1)}=0\right)\\&=P_e^{1_1}\left(1-P_e^{1_2}\right)\left(1-P_e^{1_3}\right), \quad (25)\end{aligned}$$

where $P_e^{1_1}$ is the probability of error of self-decoding at U_1, $P_e^{1_2}$ and $P_e^{1_3}$ are the probability of error for incorrect decoding of U_2 and U_3 at U_1, respectively. The probabilities $P_e^{1_1}$, $P_e^{1_2}$ and $P_e^{1_3}$ can be obtained directly by substituting the appropriate value of k and j in (9), and are given in (26), (27) and (28), respectively, where $\Upsilon_1=R_p\sqrt{h_1}/\sigma_n$.

$$P_e^{1_1}=Q\left(\Upsilon_1P_1\right). \quad (26)$$

$$P_e^{1_2}=\frac{1}{4}\left[2Q\left(\Upsilon_1P_2\right)+Q\left(\Upsilon_1\left(P_2-2P_1\right)\right)+Q\left(\Upsilon_1\left(P_2+2P_1\right)\right)\right]. \quad (27)$$

$$P_e^{1_3}=\frac{1}{8}\left[2Q\left(\Upsilon_1P_3\right)+Q\left(\Upsilon_1\left(P_3-2P_1\right)\right)+Q\left(\Upsilon_1\left(P_3+2P_1\right)\right)+Q\left(\Upsilon_1\left(P_3-2P_2\right)\right)+Q\left(\Upsilon_1\left(P_3+2P_2\right)\right)+Q\left(\Upsilon_1\left(P_3-2P_1-2P_2\right)\right)+Q\left(\Upsilon_1\left(P_3+2P_1+2P_2\right)\right)\right]. \quad (28)$$

For imperfect SIC case, the probability of error can be written using (13) as

$$\begin{aligned}&\sum_{v=2}^{4}P\left(e_1^{(v)}\left|e_2^{(v)},e_3^{(v)}\right.\right)\\&=\underbrace{P\left(e_1^{(2)}=1\right)\left[1-\left(P\left(e_2^{(2)}=1\right).P\left(e_3^{(2)}=1\right)\right)\right]}_{I_1}\\&\quad+\underbrace{P\left(e_1^{(3)}=1\right)P\left(e_2^{(3)}=1\right)\left[1-P\left(e_3^{(3)}=1\right)\right]}_{I_2}\\&\quad+\underbrace{P\left(e_1^{(4)}=1\right)P\left(e_2^{(4)}=1\right)P\left(e_3^{(4)}=1\right)}_{I_3}, \quad (29)\end{aligned}$$

where I_1 represents the probability of error of the combination when U_1, U_2 and U_3 are decoded incorrectly, correctly and incorrectly, respectively, I_2 represents the probability of error when U_1, U_2 and U_3 are decoded incorrectly, incorrectly and correctly, respectively, and I_3 represents the probability of error when U_1, U_2 and U_3 are decoded incorrectly, incorrectly and incorrectly, respectively. The derivation of I_1, I_2 and I_3 are given below.

Using (14) and (29), I_1 can be written as

$$\begin{aligned}&P\left(e_1^{(2)}=1\left|e_2^{(2)}=0,e_3^{(2)}=1\right.\right)\\&=\left[\frac{1}{4}\sum_{i=0}^{3}P\left(\widehat{y_1}\neq s_1\left|s_1^i\widehat{s_3^i}\right.\right)\right]\times\left[1-\left\{\left(\frac{1}{8}\sum_{i=0}^{7}P\left(\widehat{s_2}\neq s_2\left|s_1^is_2^i\widehat{s_3^i}\right.\right)\right)\times\left(\frac{1}{8}\sum_{i=0}^{7}P\left(\widehat{s_3}\neq s_3\left|s_1^is_2^is_3^i\right.\right)\right)\right\}\right]. \quad (30)\end{aligned}$$

By substituting the symbol values in different symbol combinations, and using direct detection method, Eq. (30) can be further solved as in (31), as shown at the bottom of the next page.

Using (14) and (29), I_2 can be written as

$$\begin{aligned}&P\left(e_1^{(3)}=1\left|e_2^{(3)}=1,e_3^{(3)}=0\right.\right)\\&=\left[\frac{1}{4}\sum_{i=0}^{3}\left(P\left(\widehat{y_1}\neq s_1\left|s_1^i\widehat{s_2^i}\right.\right)\;P\left(\widehat{s_2}\neq s_2\left|s_1^is_2^i\right.\right)\right]\times\left[1-\left(\frac{1}{8}\sum_{i=0}^{7}P\left(\widehat{s_3}\neq s_3\left|s_1^is_2^is_3^i\right.\right)\right)\right]. \quad (32)\end{aligned}$$

$$\begin{aligned}P\left(e_2^{(2)}=1\left|e_3^{(2)}=1\right.\right)=\frac{1}{8}&\left[Q\left(\Upsilon_2\left(P_2-2P_3\right)\right)Q\left(\Upsilon_2P_3\right)+Q\left(\Upsilon_2\left(P_2+2P_3\right)\right)Q\left(\Upsilon_2P_3\right)+Q\left(\Upsilon_2\left(P_2-2P_3\right)\right)Q\left(\Upsilon_2\left(P_3-2P_2\right)\right)\right.\\&+Q\left(\Upsilon_2\left(P_2+2P_3\right)\right)Q\left(\Upsilon_2\left(P_3+2P_2\right)\right)+Q\left(\Upsilon_2\left(P_2-2P_1+2P_3\right)\right)Q\left(\Upsilon_2\left(P_3-2P_1\right)\right)\\&+Q\left(\Upsilon_2\left(P_2-2P_1-2P_3\right)\right)Q\left(\Upsilon_2\left(P_3+2P_1\right)\right)+Q\left(\Upsilon_2\left(P_2+2P_1-2P_3\right)\right)Q\left(\Upsilon_2\left(P_3-2P_1-2P_2\right)\right)\\&\left.+Q\left(\Upsilon_2\left(P_2+2P_1+2P_3\right)\right)Q\left(\Upsilon_2\left(P_3+2P_1+2P_2\right)\right)\right]. \quad (23)\end{aligned}$$

By substituting the symbol values in different symbol combinations, and using direct detection method, Eq. (32) can be further solved as in (33), as shown at the bottom of the page.

Using (14) and (29), I_3 can be written as

$$P\left(e_1^{(4)}=1\,\middle|\,e_2^{(4)}=1,e_3^{(4)}=1\right)=\sum_{i=0}^{7}\left[P\left(\widehat{y_1}\neq s_1\,\middle|\,s_1^i,\widehat{s_2^i},\widehat{s_3^i}\right)P\left(\widehat{s_2^i}\neq s_2\,\middle|\,s_1^i,s_2^i,\widehat{s_3^i}\right)P\left(\widehat{s_3^i}\neq s_3\,\middle|\,s_1^i,s_2^i,s_3^i\right)P\left(s_1^i\right)P\left(s_2^i\right)P\left(s_3^i\right)\right]. \quad (34)$$

By substituting the symbol values in different symbol combinations, and using direct detection method, Eq. (34) can be further solved as in (35), as shown at the bottom of the next page, where $\xi_1 = P_1 + 2P_2 + 2P_3$, $\xi_2 = P_1 + 2P_2 - 2P_3$, $\xi_3 = P_1 - 2P_2 + 2P_3$ and $\xi_4 = P_1 - 2P_2 - 2P_3$.

V. RESULT AND DISCUSSION

The derived probability of error expressions are evaluated numerically and compared with the simulation results. Table 1 shows the system configuration and simulation parameters considered for this analysis. A three user scenario is considered where the users, i.e., U_1, U_2 and U_3 are located at the co-ordinates $(3m, 3m, 0.8m)$, $(3.5m, 1.5m, 0.8m)$ and $(1m, 1m, 0.8m)$, respectively. Fixed power allocation strategy is considered for NOMA implementation with $\alpha = 0.2$, unless otherwise stated. Since the channel gains of MU-MIMO-NOMA-VLC system are in the order of 10^{-5}, the probability of error curves will experience an offset of $100dB$ with respect to the received SNR.

In Fig. 3, the probability of error curves for a three user 2×2 MIMO-NOMA-VLC system are plotted against the SNR. The probability of error for all the three users improves as SNR increases. The error performance of U_3 is superior to that of U_1 and U_2, which is well justified as higher power is allocated to U_3 for successful SIC implementation. The figure also compares the error performance of 2×2 MIMO-NOMA-VLC system with that of single input single output (SISO) NOMA-VLC system. For SISO-NOMA-VLC system, the location co-ordinates of LED are considered as $(2.5m, 2.5m, 3m)$ and the co-ordinates of U_1, U_2 and U_3 are considered as $(3m, 3m, 0.8m)$, $(3.5m, 1.5m, 0.8m)$ and $(1m, 1m, 0.8m)$, respectively. The 2×2 MIMO-NOMA-VLC system outperforms the later given that both systems have adopted the identical power allocation strategy. The simulation results are in close agreement with that of analytical results.

In Fig. 4, the probability of error curves for a three user $M \times N$ MIMO-NOMA-VLC system is plotted against the SNR for varying M, i.e., number of PD's at each user terminal. For the analysis, system is considered with a fixed number of LED's, i.e., $N = 2$, and $M = 2, 3$ and 4. For $M = 2$, the location coordinates of PD's are given in Table 1. For the case of $M = 3$ and 4, the location coordinates of U_1, U_2 and U_3 are given in Table 2. The figure shows an improvement in error performance of U_1, U_2 and U_3 as M increases. The reason behind this improvement is the increment in equivalent channel gain at the output of MRC combiner which results from the addition of more LOS paths between the LED and PD.

In Fig. 5, the error performance of 2×2 MIMO-NOMA-VLC system is plotted against the power allocation co-efficient, α, at the SNR of $128dB$. The error performance of U_3 degrades as α increases. This degradation in error performance is due to the decrement in allocated power to U_3 as α increases. Whereas, the error performance of U_2 shows

$$P\left(e_1^{(2)}=1\,\middle|\,e_2^{(2)}=0,e_3^{(2)}=1\right)=\left[\frac{1}{2}\left(Q\left(\Upsilon_1\left(P_1+2P_3\right)\right)+Q\left(\Upsilon_1\left(P_1-2P_3\right)\right)\right)\right]\times\left[1-\left\{\left(\frac{1}{8}\left(2Q\left(\Upsilon_1\left(P_2-2P_3\right)\right)\right.\right.\right.$$
$$+2Q\left(\Upsilon_1\left(P_2+2P_3\right)\right)+Q\left(\Upsilon_1\left(P_2-2P_1+2P_3\right)\right)+Q\left(\Upsilon_1\left(P_2-2P_1-2P_3\right)\right)$$
$$\left.\left.\left.+Q\left(\Upsilon_1\left(P_2+2P_1-2P_3\right)\right)+Q\left(\Upsilon_1\left(P_2+2P_1+2P_3\right)\right)\right)\right\}\right]\times\left[\left\{\frac{1}{8}\left(2Q\left(\Upsilon_1P_3\right)\right.\right.$$
$$+Q\left(\Upsilon_1\left(P_3-2P_2\right)\right)+Q\left(\Upsilon_1\left(P_3+2P_2\right)\right)+Q\left(\Upsilon_1\left(P_3-2P_1\right)\right)+Q\left(\Upsilon_1\left(P_3+2P_1\right)\right)$$
$$\left.\left.+Q\left(\Upsilon_1\left(P_3-2P_1-2P_2\right)\right)+Q\left(\Upsilon_1\left(P_3+2P_1+2P_2\right)\right)\right)\right\}\right]. \quad (31)$$

$$P\left(e_1^{(3)}=1\,\middle|\,e_2^{(3)}=1,e_3^{(3)}=0\right)=\left[\frac{1}{4}\left(Q\left(\Upsilon_1\left(P_1+2P_2\right)\right)Q\left(\Upsilon_1P_2\right)\right)+\left(Q\left(\Upsilon_1\left(P_1-2P_2\right)\right)Q\left(\Upsilon_1P_2\right)\right)\right.$$
$$\left.+\left(Q\left(\Upsilon_1\left(P_1+2P_2\right)\right)Q\left(\Upsilon_1\left(P_2+2P_1\right)\right)\right)+\left(Q\left(\Upsilon_1\left(P_1-2P_2\right)\right)Q\left(\Upsilon_1\left(P_2-2P_1\right)\right)\right)\right]$$
$$\times\left[1-\left\{\frac{1}{8}\left(2Q\left(\Upsilon_1P_3\right)+Q\left(\Upsilon_1\left(P_3-2P_1\right)\right)+Q\left(\Upsilon_1\left(P_3+2P_1\right)\right)+Q\left(\Upsilon_1\left(P_3-2P_2\right)\right)\right.\right.$$
$$\left.\left.+Q\left(\Upsilon_1\left(P_3+2P_2\right)\right)+Q\left(\Upsilon_1\left(P_3-2P_1-2P_2\right)\right)+Q\left(\Upsilon_1\left(P_3+2P_1+2P_2\right)\right)\right)\right\}\right]. \quad (33)$$

TABLE 1. System configuration and simulation parameters for MU-MIMO-NOMA-VLC system.

	Description	Value
Set-up Parameters	Room dimension	$5m \times 5m \times 3m$
Source Parameters	No. of LED's (N)	2
	Source Co-ordinates LED 1 LED 2	 $2.5m \times 2.4m \times 3m$ $2.5m \times 2.6m \times 3m$
	Semi-half angle of LED $(\phi_{1/2})$	60°
	Inter-LED distance (D_{Tx})	$0.2m, 0.4m, 2m$
Receiver Parameters	No. of PD's (M)	2
	Near User Co-ordinates (U_1)	$PD_1(3m \times 2.95m \times 0.8m)$ $PD_2(3m \times 3.05m \times 0.8m)$
	Middle User Co-ordinates (U_2)	$PD_1(3.5m \times 1.45m \times 0.8m)$ $PD_2(3.5m \times 1.55m \times 0.8m)$
	Far User Co-ordinates (U_3)	$PD_1(1m \times 0.95m \times 0.8m)$ $PD_2(1m \times 1.05m \times 0.8m)$
	Inter-PD distance (D_{Rx})	$0.1m, 0.4m, 0.6m, 0.8m$
	Active area of PD (A_r)	$1cm^2$
	FOV (ψ_c)	60°
	Responsivity (R_p)	1 A/W
	Refractive Index (n)	1.5
	Gain of optical filter (T_s)	1
	Noise Bandwidth (W)	$50MHz$
	Transmission rate (R_b)	$50Mbps$

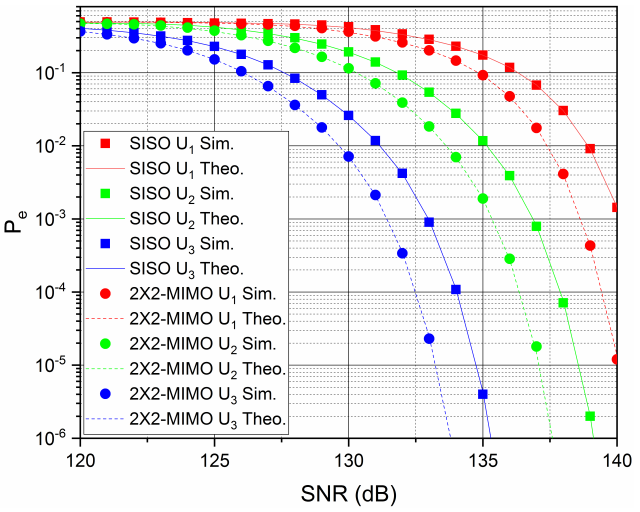

FIGURE 3. Error performance of three user 2 × 2 MIMO-NOMA-VLC system.

TABLE 2. PD locations of U_1, U_2 and U_3.

Users	$M = 3$	$M = 4$
U_1	$PD_1(3m, 2.9m, 0.8m)$ $PD_2(3m, 3m, 0.8m)$ $PD_3(3m, 3.1m, 0.8m)$	$PD_1(3m, 2.85m, 0.8m)$ $PD_2(3m, 2.95m, 0.8m)$ $PD_3(3m, 3.05m, 0.8m)$ $PD_4(3m, 3.15m, 0.8m)$
U_2	$PD_1(3.5m, 1.4m, 0.8m)$ $PD_2(3.5m, 1.5m, 0.8m)$ $PD_3(3.5m, 1.6m, 0.8m)$	$PD_1(3.5m, 1.35m, 0.8m)$ $PD_2(3.5m, 1.45m, 0.8m)$ $PD_3(3.5m, 1.55m, 0.8m)$ $PD_4(3.5m, 1.65m, 0.8m)$
U_3	$PD_1(1m, 0.9m, 0.8m)$ $PD_2(1m, 1m, 0.8m)$ $PD_3(1m, 1.1m, 0.8m)$	$PD_1(1m, 0.85m, 0.8m)$ $PD_2(1m, 0.95m, 0.8m)$ $PD_3(1m, 1.05m, 0.8m)$ $PD_4(1m, 1.15m, 0.8m)$

an improvement for $\alpha \leq 0.3$ and thereafter, it degrades as α increases beyond 0.3 i.e., $\alpha > 0.3$. Though, the power allocated to U_2 increases as α increases, it does not lead to performance improvement in U_2 at $\alpha > 0.3$. This is because at this range of α, the power allocated to U_3 become low which results in the failure of SIC at U_2 and subsequent performance degradation in U_2. The similar trend can also be seen for U_1 around the power allocation co-efficient of 0.35. Moreover, the justification provided for U_2 is also valid for U_1. The figure demonstrates that on an average, the proposed system offers best performance at $\alpha = 0.3$.

The error performance of a three user 2×2 MIMO-NOMA-VLC system is shown in Fig. 6 for different values of D_{Tx}, i.e., distance between the two LEDs. In particular, three values

$$P\left(e_1^{(4)}=1 \,\middle|\, e_2^{(4)}=1, e_3^{(4)}=1\right) = \frac{1}{8}\Big[Q\left(\Upsilon_1\left(\xi_1\right)\right)Q\left(\Upsilon_1\left(P_2+2P_3\right)\right)Q\left(\Upsilon_1 P_3\right)+Q\left(\Upsilon_1\left(\xi_2\right)\right)Q\left(\Upsilon_1\left(P_2-2P_3\right)\right)Q\left(\Upsilon_1 P_3\right)$$
$$+Q\left(\Upsilon_1\left(\xi_3\right)\right)Q\left(\Upsilon_1\left(P_2-2P_3\right)\right)Q\left(\Upsilon_1\left(P_3-2P_2\right)\right)+Q\left(\Upsilon_1\left(\xi_4\right)\right)Q\left(\Upsilon_1\left(P_2+2P_3\right)\right)$$
$$Q\left(\Upsilon_1\left(P_3+2P_2\right)\right)+Q\left(\Upsilon_1\left(\xi_4\right)\right)Q\left(\Upsilon_1\left(P_2-2P_1+2P_3\right)\right)Q\left(\Upsilon_1\left(P_3-2P_1\right)\right)+Q\left(\Upsilon_1\left(\xi_3\right)\right)$$
$$Q\left(\Upsilon_1\left(P_2-2P_1-2P_3\right)\right)Q\left(\Upsilon_1\left(P_3+2P_1\right)\right)+Q\left(\Upsilon_1\left(\xi_2\right)\right)Q\left(\Upsilon_1\left(P_2+2P_1-2P_3\right)\right)$$
$$Q\left(\Upsilon_1\left(P_3-2P_1-2P_2\right)\right)+Q\left(\Upsilon_1\left(\xi_1\right)\right)Q\left(\Upsilon_1\left(P_2+2P_1+2P_3\right)\right)Q\left(\Upsilon_1\left(P_3+2P_1+2P_2\right)\right)\Big]. \quad (35)$$

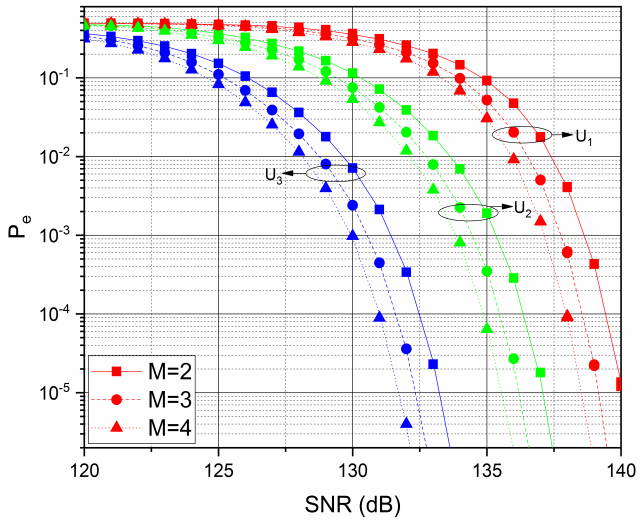

FIGURE 4. Error performance of three user $M \times N$ MIMO-NOMA-VLC system with increasing M.

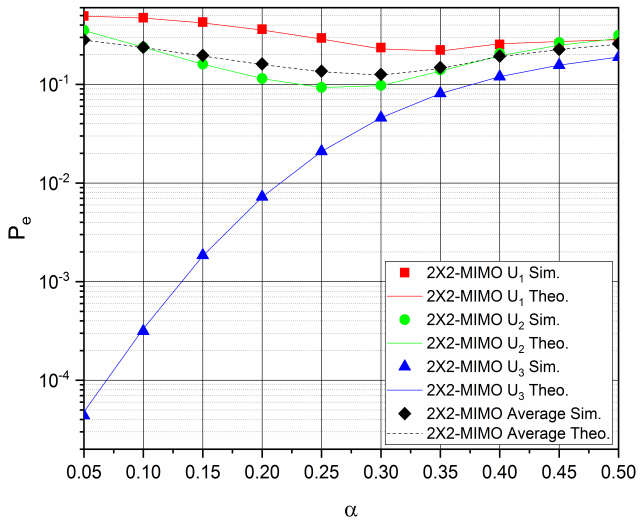

FIGURE 5. Probability of error vs. α curves for a three user 2 × 2 MIMO-NOMA-VLC system.

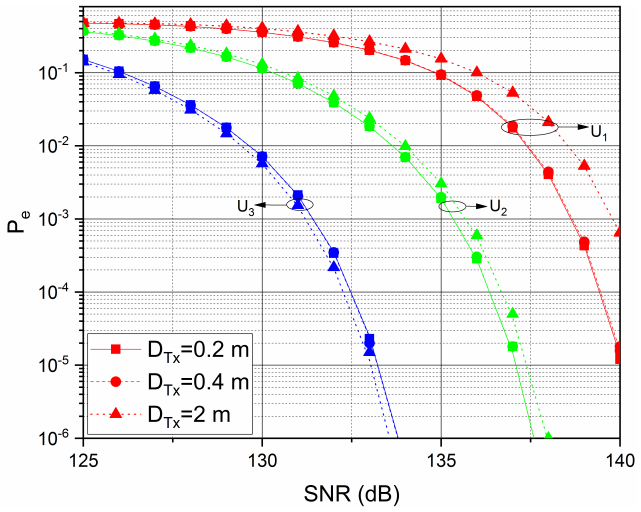

FIGURE 6. Error performance of three user 2 × 2 MIMO-NOMA-VLC system for different values of D_{Tx}.

TABLE 3. Effect Of D_{Rx} on the error performance of 2 × 2 MIMO-NOMA-VLC System.

SNR (in dB)	U_k	P_e			
		(D_{Rx}) =0.1m	(D_{Rx}) =0.4m	(D_{Rx}) =0.6m	(D_{Rx}) =0.8m
125	U_1	0.475203	0.475442	0.475762	0.476211
	U_2	0.36538	0.364538	0.363527	0.362312
	U_3	0.151899	0.149558	0.146602	0.142761
130	U_1	0.356044	0.357487	0.359429	0.362176
	U_2	0.114507	0.113557	0.112424	0.111074
	U_3	0.007223	0.006877	0.006455	0.005932
135	U_1	0.092298	0.09396	0.096223	0.099479
	U_2	0.001907	0.001848	0.00178	0.0017
	U_3	9.71E-10	6.76E-10	4.23E-10	2.24E-10

of D_{Tx}, i.e., $D_{Tx} = 0.2m, 0.4m, 2m$, are considered for performance investigation. The figure shows that the probability of error of U_3 improves whereas, the probability of error of U_1 and U_2 degrades as D_{Tx} increases. It is to be noted that increment/decrement in D_{Tx} results in the change in location coordinates of transmitting LEDs and consequently, the channel gains between LEDs and PDs are affected. However, a significant change in error performance can only be observed when D_{Tx} is sufficiently large.

Table 3 investigates the effect of D_{Rx}, i.e., distance between PDs at each user, on the error performance of three user 2×2 MIMO-NOMA-VLC system. For analysis purpose, four different values of D_{Rx}, i.e., $D_{Rx} = 0.1m$, $0.4m$, $0.6m$ and $0.8m$, are considered. The probability of error values given in Table depicts that the error performance of the users except U_1 improve when D_{Rx} increases. Further, at a given SNR, U_3 shows best performance followed by U_2 and U_1. Furthermore, the performance of the system improves as SNR increases.

Fig. 7 compares the performance of proposed three user 2×2 MIMO-NOMA-VLC system with SISO-NOMA-VLC system of [16]. For the comparison, the system model of [16] is adopted, and accordingly, the co-ordinates of LEDs and PDs of MIMO-NOMA-VLC system are redefined. Specifically, for 2×2 MIMO-NOMA-VLC system, the location coordinates of LEDs are considered as $(2m \times 1.95m \times 3m)$ and $(2m \times 2.05m \times 3m)$, and the location coordinates of PDs for U_1, U_2 and U_3 are considered to be $PD_1\,(2.3m \times 2.25m \times 1.25m)$ and $PD_2\,(2.3m \times 2.35m \times 1.25m)$, $PD_1(2.4m \times 2.35m \times$

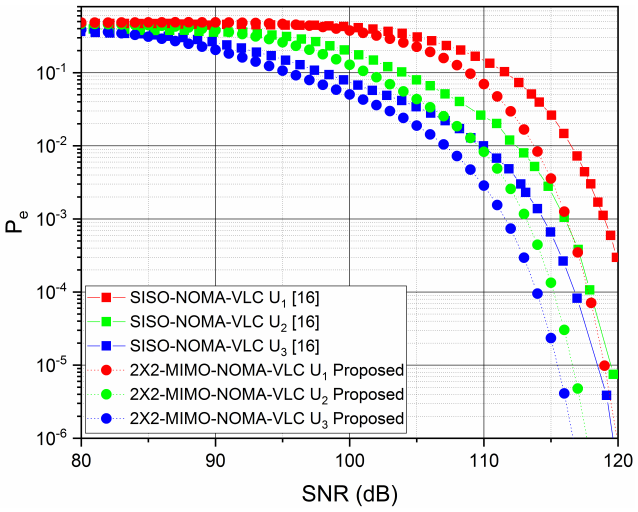

FIGURE 7. Error performance comparison of proposed three user 2 × 2 MIMO-NOMA-VLC system with SISO-NOMA-VLC system of [16].

$1.25m$) and PD_2 ($2.4m \times 2.45m \times 1.25m$) , and PD_1 ($2.5m \times 2.45m \times 1.25m$) and PD_2 ($2.5m \times 2.55m \times 1.25m$) , respectively. The figure shows that the proposed 2×2 MIMO-NOMA-VLC system completely outperforms the SISO-NOMA-VLC system presented in [16]. Further, the figure shows that the error performance of U_3 is superior to that of U_1 and U_2 for both the systems.

VI. CONCLUSION

In this paper the error performance of MU-MIMO-NOMA-VLC system is analyzed in the presence of perfect and imperfect SIC. In particular, RC and MRC techniques are adopted at the transmitter and receiver, respectively, in order to improve the performance of NOMA-VLC system. The closed form expressions for the probability of error of the MU-MIMO-NOMA-VLC users are derived over LOS channel. It is concluded that a three user 2×2 MIMO-NOMA-VLC system outperforms the SISO-NOMA-VLC system with same set of parameters. Further, an improvement in the error performance of a three user $M \times N$ MIMO-NOMA-VLC system is observed as number of PDs, i.e., M, increases. Furthermore, the best error performance of a three user 2×2 MIMO-NOMA-VLC system is observed at $\alpha = 0.3$, however, beyond this range of α, the error performance of the system deteriorates significantly. It is also concluded that a significant improvement/degradation in the error performance of the users is observed only at large D_{Tx}. On the contrary, the variation in D_{Rx} does not has much effect on the error performance of the users.

REFERENCES

[1] *Cisco Annual Internet Report, 2018–2023 White Paper*, Cisco, San Jose, CA, USA, 2020.

[2] Z. Ghassemlooy, W. Popoola, and S. Rajbhandari, *Optical Wireless Communications: System and Channel Modeling With MATLAB*, 1st ed. New York, NY, USA: CRC Press, 2013.

[3] D. C. O'Brien, L. Zeng, H. Le-Minh, G. Faulkner, J. W. Walewski, and S. Randel, "Visible light communications: Challenges and possibilities," in *Proc. IEEE 19th Int. Symp. Pers., Indoor Mobile Radio Commun.*, Sep. 2008, pp. 1–5.

[4] H. Le Minh, Z. Ghassemlooy, D. O'Brien, and G. Faulkner, "Indoor gigabit optical wireless communications: Challenges and possibilities," in *Proc. 12th Int. Conf. Transparent Opt. Netw.*, Jun. 2010, pp. 1–6.

[5] P. H. Pathak, X. Feng, P. Hu, and P. Mohapatra, "Visible light communication, networking, and sensing: A survey, potential and challenges," *IEEE Commun. Surveys Tuts.*, vol. 17, no. 4, pp. 2047–2077, 4th Quart., 2015.

[6] V. Dixit, S. Shukla, and M. Shukla, "Performance analysis of optical IDMA system for indoor wireless channel model," in *Proc. 4th Int. Conf. Comput. Intell. Commun. Netw.*, Nov. 2012, pp. 382–386.

[7] M. Takahashi, K. Shimada, K. Maruta, and C.-J. Ahn, "Throughput improvement using code length optimization for VLC-OFDM/IDMA," in *Proc. Int. Conf. Adv. Technol. Commun. (ATC)*, Oct. 2019, pp. 33–37.

[8] L. Dai, B. Wang, Y. Yuan, S. Han, I. Chih-lin, and Z. Wang, "Non-orthogonal multiple access for 5G: Solutions, challenges, opportunities, and future research trends," *IEEE Commun. Mag.*, vol. 53, no. 9, pp. 74–81, Sep. 2015.

[9] S. M. R. Islam, N. Avazov, O. A. Dobre, and K.-S. Kwak, "Power-domain non-orthogonal multiple access (NOMA) in 5G systems: Potentials and challenges," *IEEE Commun. Surveys Tuts.*, vol. 19, no. 2, pp. 721–742, 2nd Quart., 2017.

[10] P. Sharma, A. Kumar, and M. Bansal, "Performance analysis of downlink NOMA over $\eta - -\mu$ and $\kappa - -\mu$ fading channels," *IET Commun.*, vol. 14, no. 3, pp. 522–531, Feb. 2020, doi: 10.1049/IET-com.2019.0413.

[11] Z. Ding, P. Fan, and H. V. Poor, "Impact of user pairing on 5G non-orthogonal multiple-access downlink transmissions," *IEEE Trans. Veh. Technol.*, vol. 65, no. 8, pp. 6010–6023, Aug. 2016, doi: 10.1109/TVT.2015.2480766.

[12] L. Yin, X. Wu, and H. Haas, "On the performance of non-orthogonal multiple access in visible light communication," in *Proc. IEEE 26th Annu. Int. Symp. Pers., Indoor, Mobile Radio Commun. (PIMRC)*, Aug. 2015, pp. 1354–1359.

[13] B. Lin, X. Tang, Z. Ghassemlooy, C. Lin, M. Zhang, Z. Zhou, Y. Wu, and H. Li, "A NOMA scheme for visible light communications using a single carrier transmission," in *Proc. 1st South Amer. Colloq. Visible Light Commun. (SACVLC)*, Nov. 2017, pp. 1–4.

[14] E. M. Almohimmah and M. T. Alresheedi, "Error analysis of NOMA-based VLC systems with higher order modulation schemes," *IEEE Access*, vol. 8, pp. 2792–2803, 2020.

[15] X. Liu, Z. Chen, Y. Wang, F. Zhou, Y. Luo, and R. Q. Hu, "BER analysis of NOMA-enabled visible light communication systems with different modulations," *IEEE Trans. Veh. Technol.*, vol. 68, no. 11, pp. 10807–10821, Nov. 2019.

[16] H. Marshoud, P. C. Sofotasios, S. Muhaidat, G. K. Karagiannidis, and B. S. Sharif, "Error performance of NOMA VLC systems," in *Proc. IEEE Int. Conf. Commun. (ICC)*, May 2017, pp. 1–6, doi: 10.1109/ICC.2017.7996769.

[17] V. Dixit and A. Kumar, "An exact BER analysis of NOMA-VLC system with imperfect SIC and CSI," *AEU Int. J. Electron. Commun.*, vol. 138, Aug. 2021, Art. no. 153864, doi: 10.1016/j.aeue.2021.153864.

[18] C. Chen, W. Zhong, H. Yang, P. Du, and Y. Yang, "Flexible-rate SIC-free NOMA for downlink VLC based on constellation partitioning coding," *IEEE Wireless Commun. Lett.*, vol. 8, no. 2, pp. 568–571, Apr. 2019, doi: 10.1109/LWC.2018.2879924.

[19] L. Zeng, D. O'Brien, H. Minh, G. Faulkner, K. Lee, D. Jung, Y. Oh, and E. T. Won, "High data rate multiple input multiple output (MIMO) optical wireless communications using white led lighting," *IEEE J. Sel. Areas Commun.*, vol. 27, no. 9, pp. 1654–1662, Dec. 2009.

[20] V. Dixit and A. Kumar, "Performance analysis of angular diversity receiver based MIMO-VLC system for imperfect CSI," *J. Optic*, vol. 23, no. 8, 2021, Art. no. 085701, doi: 10.1088/2040-8986/ac1321.

[21] T. Fath and H. Haas, "Performance comparison of MIMO techniques for optical wireless communications in indoor environments," *IEEE Trans. Commun.*, vol. 61, no. 2, pp. 733–742, Feb. 2013.

[22] C. Chen, W.-De Zhong, H. Yang, and P. Du, "On the performance of MIMO-NOMA-based visible light communication systems," *IEEE Photon. Technol. Lett.*, vol. 30, no. 4, pp. 307–310, Feb. 15, 2018.

[23] R. Mitra and V. Bhatia, "Precoded chebyshev-NLMS-based pre-distorter for nonlinear LED compensation in NOMA-VLC," *IEEE Trans. Commun.*, vol. 65, no. 11, pp. 4845–4856, Nov. 2017.

[24] V. Dixit and A. Kumar, "Performance analysis of non-line of sight visible light communication systems," *Opt. Commun.*, vol. 459, Mar. 2020, Art. no. 125008.
[25] V. Dixit and A. Kumar, "Performance analysis of L-PPM modulated NLOS-VLC system with perfect and imperfect CSI," *J. Optic*, vol. 23, no. 1, 2020, Art. no. 015702.
[26] J. R. Barry, J. M. Kahn, W. J. Krause, E. A. Lee, and D. G. Messerschmitt, "Simulation of multipath impulse response for indoor wireless optical channels," *IEEE J. Sel. Areas Commun.*, vol. 11, no. 3, pp. 367–379, Apr. 1993.
[27] M. Safari and M. Uysal, "Do we really need OSTBCs for free-space optical communication with direct detection?" *IEEE Trans. Wireless Commun.*, vol. 7, no. 11, pp. 4445–4448, Nov. 2008.
[28] V. Dixit and A. Kumar, "Performance analysis of indoor visible light communication system with angle diversity transmitter," in *Proc. IEEE 4th Conf. Inf. Commun. Technol. (CICT)*, Dec. 2020, pp. 1–5.

VIPUL DIXIT (Student Member, IEEE) received the Bachelor of Technology degree in electronics and communication engineering and the M.Tech. degree in communication engineering from Uttar Pradesh Technical University, Lucknow, India, in 2008 and 2012, respectively. He is currently pursuing the Ph.D. degree in communication engineering with PDPM-IIITDMJ, Jabalpur, India. He is currently the Vice-Chair of the IEEE Student Branch, PDPM-IIITDMJ. His current research interests include visible light communication (VLC), non-orthogonal multiple access (NOMA), interleave division multiple access (IDMA), multiple input multiple output (MIMO) systems, diversity schemes, and imperfect channel.

ATUL KUMAR (Member, IEEE) received the Bachelor of Technology degree in electronics and communication engineering from Uttar Pradesh Technical University, Lucknow, India, in 2008, the M.Tech. degree in telecommunication engineering from the National Institute of Technology Durgapur, India, in 2010, and the Ph.D. degree in electronics and communication engineering from the Indian Institute of Technology Guwahati, India, in 2016. He has been a Faculty Member with the Department of Electronics and Communication Engineering, National Institute of Technology Jamshedpur, India. He is currently working as an Assistant Professor with the Department of Electronics and Communication Engineering, PDPM-IIITDMJ, Jabalpur, India. His research interests include chaotic digital communications, cooperative communications, multiple input multiple output (MIMO) systems, visible light communication (VLC), and non-orthogonal multiple access (NOMA).